# Wire Mesh Tension Testing

Report on Mechanical Properties of Wire Mesh Materials for Soil Stabilization Applications


Prepared By:

D. K. Anderson

B. P. Wham

Center for Infrastructure, Energy, and Space Testing

Civil, Environmental, and Architectural Engineering

University of Colorado Boulder

Boulder, CO 80309



July 2019

Dept. of Civil, Environmental & Architectural Engineering
College of Engineering and Applied Science
428 UCB
Boulder, Colorado 80309-0428
t: 303.492.8221
CIEST@colorado.edu
website:www.colorado.edu/center/ciest

## Table of Contents



## List of Figures

## List of Tables

Dept. of Civil, Environmental & Architectural Engineering
College of Engineering and Applied Science
428 UCB
Boulder, Colorado 80309-0428
t: 303.492.8221
CIEST@colorado.edu
website:www.colorado.edu/center/ciest

## 1. Introduction

This report presents results from series of 28 tension tests performed on wire mesh used for slope stabilization applications. Herein, five mesh types were tested in both the transverse and longitudinal orientations. The project was undertaken by the Center for Infrastructure, Energy, and Space Testing (CIEST) at University of Colorado Boulder.

## 2. Background

Soil stability can be enhanced through the insertion of reinforcement into the soil to resist destabilizing shear forces developed along steep slopes. A common method of increasing soil stability is the use of fully grouted soil nails set at fixed intervals over a slope. While the nails, typically 20 ft (5 m) in length, stabilize the slope at the macro scale, local soil erosion is not prevented between nails. To mitigate potential localized instability, a coverage material can be applied over the slope. Traditionally, spray-on concrete has been utilized as a coverage material, providing a wall-like structure actively preventing the erosion of the soil through a complete coverage of the hillside. An alternative method of coverage is the use of wire mesh to interconnect soil nails, known as a flexible facing system, an example of which is shown in Figure 1. Compared to a solid-facing system, flexible facing has a reduced construction time while also allowing grasses and shrubs to grow along the slope, enhancing the aesthetics and natural stability of the system.

In the flexible facing system, the mesh is placed along the slope and nails are inserted through mesh openings with typical vertical and horizontal spacing of 5 ft (1.5 m) with rows of nails offset from each other. Due to the flexibility of the wire mesh, there are no normal forces initially developed throughout the mesh to prevent localized instabilities and a mesh can be raised above the soil by simply pulling by hand. This passive system permits the soil to erode and forms bulges of displaced soil above each nail, restricted by normal forces of the mesh developed as the mesh displaces. The resisting forces that develop are dependent on the strength of the mesh and interaction of the mesh with the soil nail while the stiffness of the system is dependent on the spacing of nails and the stiffness of the wire mesh.

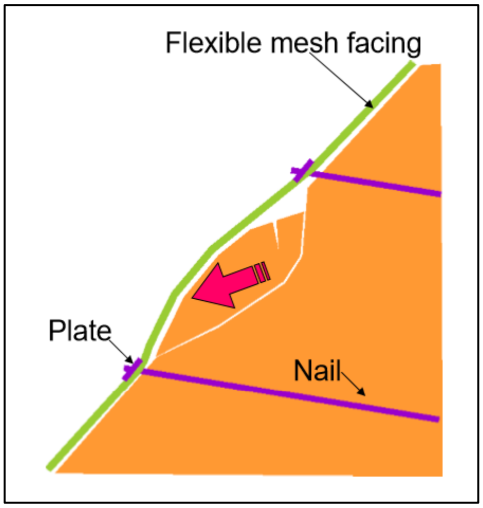


Figure 1. Flexible facing system section view (Maccaferri)

Due to the system design, an increased displacement needed to engage the resisting force developed by the mesh leads to an increased loading as more soil is permitted to erode.

As the flexible facing system does not develop stresses throughout the system upon construction, displacements needed to develop resisting forces begin at a near-zero stress level. To properly compare mesh products of different geometry and wire strengths, accurate information is needed on both the strength of the mesh and displacements needed to develop that strength value.

Wire mesh specific to the application of soil stabilization has been developed over time with variances in mesh geometry, individual wire strength, and number of twists found in the node of wire connections, but a guiding standard of testing material characteristics specific to this classification of mesh has not been developed. ASTM A 975, the wire products testing standard of the United States, is a prevalent standard referenced in the certification of soil stabilization mesh but testing methods do not accurately represent loading cases described in the flexible facing system. Testing methods under this standard require a pretension value of 20% of the anticipated failure load before measuring displacement data. The European wire products testing standard, EN 10223-3, has a lower pretension value of 899lb (4000N), but is rarely cited for strength testing in manufacturer data sheets.

Previous testing of wire mesh has predominantly been completed by mesh manufacturers, although testing methods and data are not publicly available. Third-party testing has been completed by the Wood Materials and Engineering Laboratory at Washington State University (WMEL) as part of a study into the guidelines of flexible facing system design. Multiple mesh types were tested under the same testing methods with samples of approximately 4 x 4 ft were tested under guidance of ASTM A975 and material properties of ultimate tensile strength and modulus of elasticity (lbs/in) were reported. It should be noted that the intent of this testing was not the direct comparison of mesh characteristics between products, but to verify finite element models used to study flexible facing system components.

Ruegger Systems has conducted a series of field tests to determine strength characteristics of Geobrugg Tecco G65 mesh under realistic loading conditions (Flum, 2002). The mesh was placed within a large frame of approximately 14 ft (4.27 m) square and restrained to the frame through a cable connection that attached to the frame at the corners. This test method allowed for displacement along boundary edges while providing rigid displacement boundaries at corners representing the firm boundaries of soil nails. No other mesh types were tested under these conditions.

Finite element modeling of single-twist wire mesh under static loading has been conducted by J.J. del Coz Diaz and found to be in agreeance with experimental test results (Diaz, 2009).

While strength data collected under current wire product testing standard can be used in comparing mesh for use in flexible facing systems, relevant displacement data is not currently available. This report strives to compare the material characteristics of common wire mesh used in the application of soil stabilization under identical loading conditions, providing engineers a basis for selection of an appropriate mesh for a given project. Results of testing are also compared with manufacturer reported characteristics and results of previous testing.

## 3. Test Specimens

Twenty-eight tension tests on five different wire mesh types, used for slope stabilization applications, were conducted in both the transverse and longitudinal orientations. CIEST received three shipments of wire mesh for a total of five rolls measuring 12 ft (3.66 m) square, and tested as described below. Testing standards of ASTM A 975 *Standard Specification for Double-Twisted Hexagonal Mesh Gabions and Revet Mattresses (Metallic-Coated Steel Wire or Metallic-Coated Steel Wire with Poly (Vinyl Chloride) (PVC) Coating)* (2016) and EN 10223-3 *Steel Wire and Wire Products for Fencing and Netting – Hexagonal Steel Wire Mesh Products for Civil Engineering Purposes* (2013) were considered in the testing design and used as a general guideline. Specimens were cut to shape from the material provided. Each specimen was measured to be ten (10) cells wide by four (4) cells high with the cut ends bent back to prevent the unraveling of the specimen. The orientation of a specimen was determined from the sample data sheets provided. Table 1 provides descriptions of all test specimens and the certified tensile strength if known. The testing design can be viewed in Figure 2.

## 4. Testing Methods

Based on the testing methods described in EN 10223-3, the testing apparatus shown in Figure 3a was designed and fabricated. The purpose of the apparatus design was to test the tensile strength capacities of each specimen along the perpendicular edge of loading along a row of seven (7) cells for each mesh type. Due to the differing cell dimensions of each mesh, the width of the testing plane varies with each specimen. Bolt placements along the length of each apparatus pair align with the node points of each mesh, allowing for a uniform tension load to be applied across the testing plane without deforming mesh geometry. An internal spacing between apparatus members was maintained during each test to minimize contact between the testing apparatus and wire mesh, as shown in Figure 3b. The testing apparatus was then placed into an MTS Load Frame with 490-kN (110-kip) capacity, 150-mm (6-inch) stroke, and controlled with a custom designed LabVIEW program. Both load and displacement data were recorded directly from the MTS Load Frame.

Table 1. Description and Dimensions of Tested Specimens

| **Specimen** | **Description** | **Single-Cell Dimensions ($L_{1C}$ x $B_{1c}$) in. [mm]** | **Mesh Depth in. [mm]** | **Wire Strength ksi [MPa]** | **Reported Minimum Tensile Strength lb/ft [kN/m]** |
|---|---|---|---|---|---|
| R01S | Soil Stabilization Mesh, standard orientation | 3 x 2 [76 x 50.8] | 0.71 [18] | 105-138 [724-951] | N/A |
| R01R | Soil Stabilization Mesh, rotated orientation | 2 x 3 [50.8 x 76] | 0.71 [18] | 105-138 [724-951] | N/A |
| M01S | Maccaferri GALMAC-Coated Terramesh, standard orientation | 5.67 x 3.26 [144 xx 88] | 0.12 [3] | 75 [515] | 3425 [50] |
| M01R | Maccaferri GALMAC-Coated Terramesh, rotated orientation | 3.26 x 5.67 [88 x 144] | 0.12 [3] | 75 [515] | 1800 [26.2] |
| T01S | Geobrugg Tecco G65, standard orientation | 5.63 x 3.26 [143 x 88] | 0.43 [11] | 256 [1770] | 10,200 [150] |
| T01R | Geobrugg Tecco G65, rotated orientation | 3.26 x 5.63 [88 x 143] | 0.43 [11] | 256 [1770] | N/A |
| H01S | Trumer HPN+, standard orientation | 3.73 x 3.40 [94 x 86] | 0.79 [20] | 257 [1770] | 10278 [150] |
| H01R | Trumer HPN+, rotated orientation | 3.40 x 3.73 [86 x 94] | 0.79 [20] | 257 [1770] | N/A |
| S03S | Trumer Sigma, standard orientation | 2.90 x 3.10 [74 x 79] | 0.67 [17] | 257 [1770] | 10278 [150] |
| S03R | Trumer Sigma, rotated orientation | 3.1 x 2.9 [79 x 74] | 0.67 [17] | 257 [1770] | N/A |

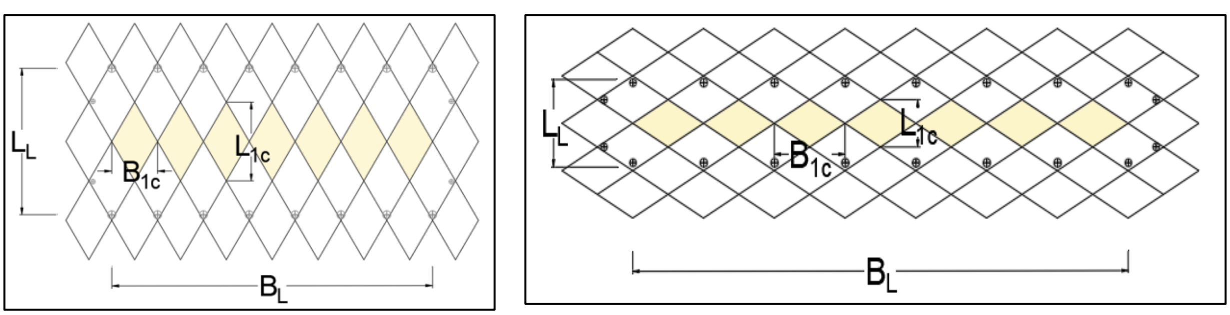


(a) (b)

Figure 2. Tension test assembly setup showing loading points of assembly with tested cells highlighted in (a) standard orientation and (b) rotated orientation (Geobrugg Tecco shown for illustration)

(a) (b)

Figure 3. Tension test assembly setup showing (a) front view and (b) side view of assembly (Geobrugg Tecco shown)


(a) T01S (b) T01R

Figure 4. Typical test configuration for standard and rotated loading

Due to constraints of the test design, specimen types were tested either at a loading length of a single cell or three cells. To ensure comparison across mesh types was still valid, Soil Stabilization Mesh was tested at both loading lengths and compared. The load vs displacement plot of the single cell test correlates strongly with that of the three-cell loading length (Figure 5). UTL does show a decline of approximately 12% from an average of 7940 lbs/ft (115 kN/m) recorded at the three-cell loading length to 7000 lbs/ft (102 kN/m) at the three-cell loading length. Failure patterns were consistent across loading lengths as described in the failure methods section below.

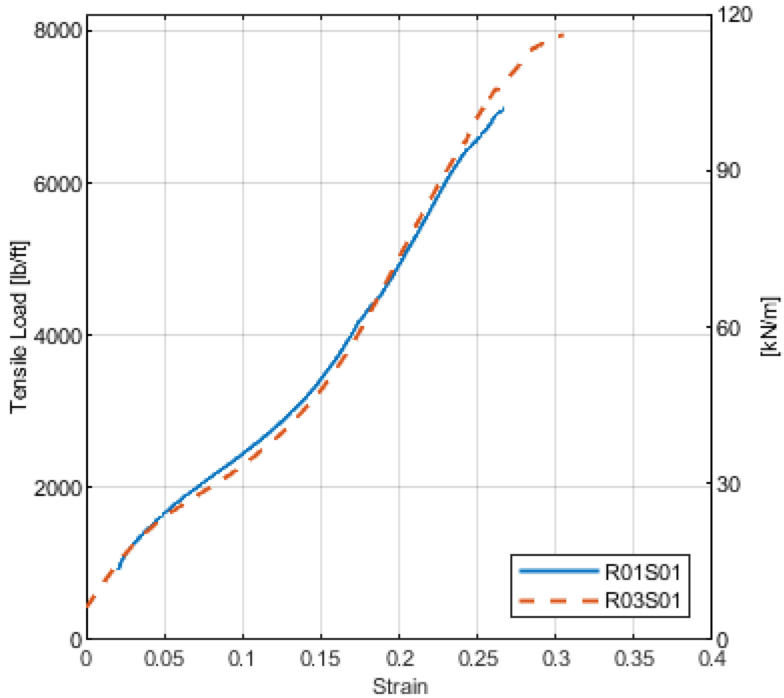


Figure 5. SSM Single Cell Versus Three Cell Testing

## 5. Test Results

The following sections provide results for the five steel meshes tested. The horizontal axis of each figure is the strain reported as the change in actuator displacement from initial prestress value divided by the specimen loading length, $L_{L.}$ The vertical axis provides measured change in load divided by the representative 7-cell loading width, $B_{L,}$ for each specimen (values reported in Table 1 and depicted in Figure 2). Data is displayed from the initial preloading until the Ultimate Tensile Load (UTL). Prestress of the specimen is reported as 400 lb/ft (5.84 kN/m) loading and was determined as the minimum loading across all specimen in which inconsistencies in loading data were not present. Data collected before the prestress loading is not considered in modulus of elasticity calculations. Specified minimum strengths described in Table 1 have been plotted as a threshold without a corresponding strain measurement for each mesh. Tests R03R01, M01S01, M01R01, T01S01, and T01R01 were completed with a prestress value of 20% of the anticipated UTL as suggested in ASTM A975 and therefore strain data below that threshold was not recorded. This data has been adjusted by setting the initial strain values measured at the 20% prestress threshold with strains of equal stress of redundant tests in which all test data was recorded.

### 5.1. *Soil Stabilization Mesh Tension Test Results*

Soil Stabilization Mesh (SSM) specimens were tested at a 3-cell loading length and Figure 6 presents the test data for both orientations. The reduction of stiffness of the specimen beginning at 0.12 strain for standard oriented specimen and 0.24 strain for rotated oriented specimen is attributed to the geometry of the mesh. Stiffness below these thresholds consists of the deformation along the axis perpendicular to the axis of loading combined with deformation normal to the mesh face provided by the width of the specimen. Above these thresholds the mesh specimen has reached the deformed shape normal to the axis of loading and deformation predominantly occurs parallel to the loading axis. Photos of the mesh cross section can be viewed in the Appendix.

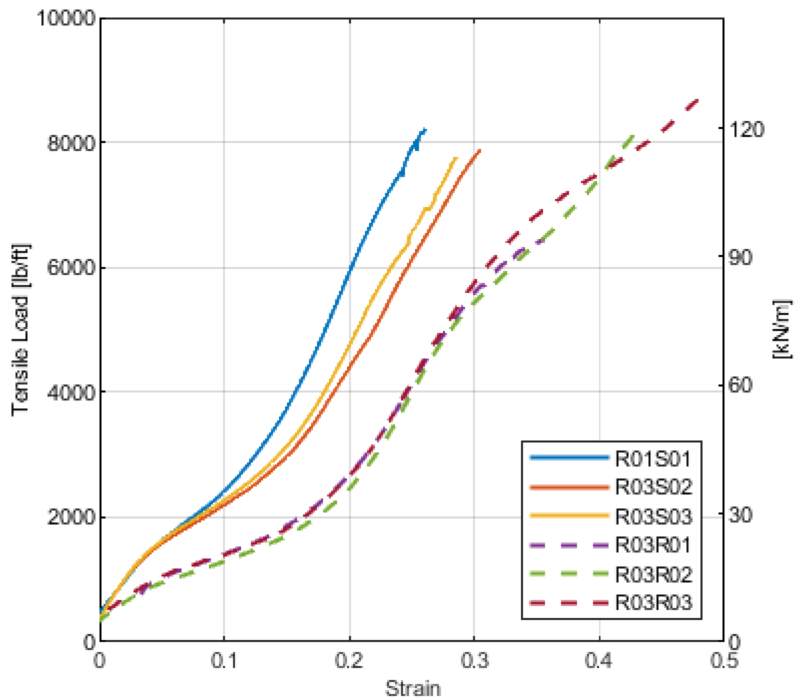


Figure 6. Soil Stabilization Mesh load vs displacement

Dept. of Civil, Environmental & Architectural Engineering
College of Engineering and Applied Science
428 UCB
Boulder, Colorado 80309-0428
t: 303.492.8221
CIEST@colorado.edu
website:www.colorado.edu/center/ciest

### 5.2. *Maccaferri Tension Test Results*

Figure 7 shows results from the Maccaferri Doubletwist (Doubletwist) mesh tests, tested at a 1-cell loading length. The consistent stiffness throughout loading can be attributed to the minimal depth of the mesh by eliminating displacement normal to the plane of loading. Without deformation along the axis normal to the mesh face, there is not a mechanism to provide a large change in stiffness.

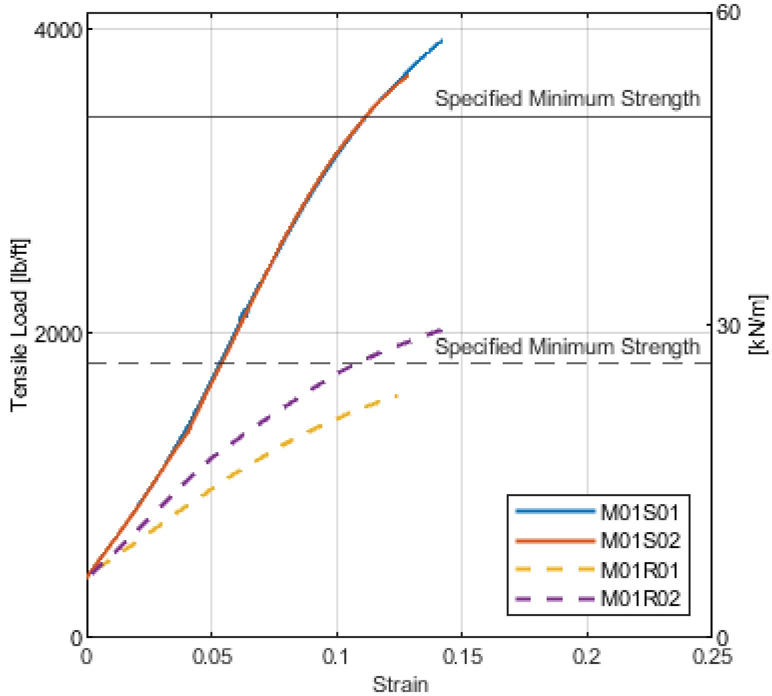


Figure 7. Maccaferri Doubletwist load versus displacement

### 5.3. *Geobrugg Tecco G65 Tension Test Results*

Figure 8 shows results from Geobrugg Tecco G65 (Tecco) specimens, tested at a 1-cell loading length. The slender depth of Tecco mesh combined with high curvature only found within the nodes, leads to minimal displacement along the axis normal to the face of the mesh. While completing the T01R01 test, yielding occurred at the outside boundary restraints, reducing the effects of the outer boundary condition. Validation tests were completed with improved restraints and it was found that the corresponding initial failure locations did not represent the UTL. The initial failure was located at the outer boundary restraint while the secondary failure was located at the wire leading to the inner boundary restraint and corresponded to the UTL. Further investigation is discussed in the Failure Methods section.

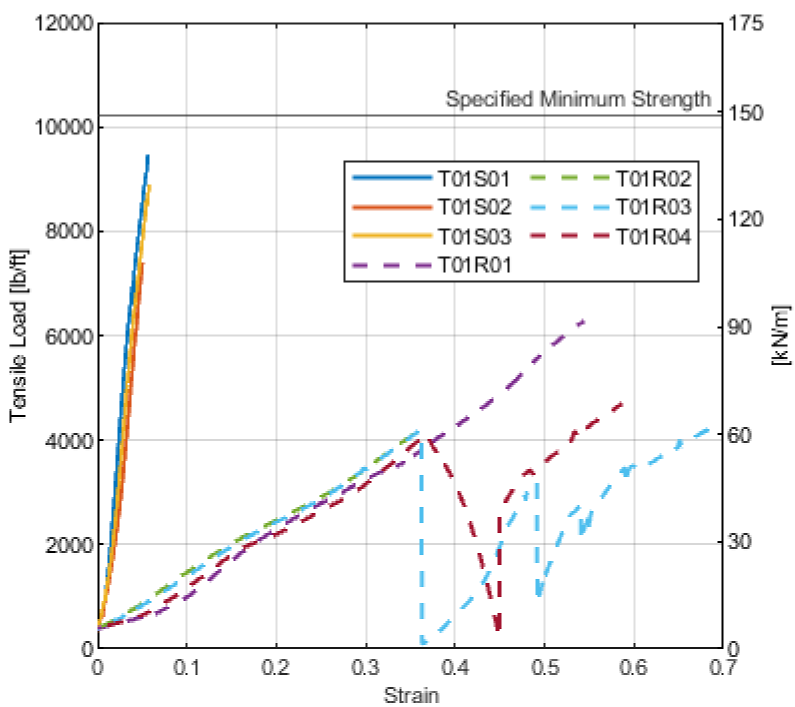


Figure 8. Geobrugg Tecco load vs displacement

Dept. of Civil, Environmental & Architectural Engineering
College of Engineering and Applied Science
428 UCB
Boulder, Colorado 80309-0428
t: 303.492.8221
CIEST@colorado.edu
website:www.colorado.edu/center/ciest

### 5.4. *Trumer HPN+ Tension Test Results*

Trumer HPN+ (HPN) specimens were tested at a 1-cell loading length and Figure 9 presents the test data for both orientations. All tests completed passed specified minimum strength thresholds. While HPN mesh has the largest depth of all mesh tested, a change in stiffness is not apparent due to the thickness in wire accounting for a large portion of the depth. Reduction in stiffness found in rotated orientation mesh found at 0.9 strain and again at 0.36 strain can be attributed to the vertical orientation of continuous wires slipping and allowing for more displacement when compared to the standard orientation with continuous wires in a horizontal orientation.

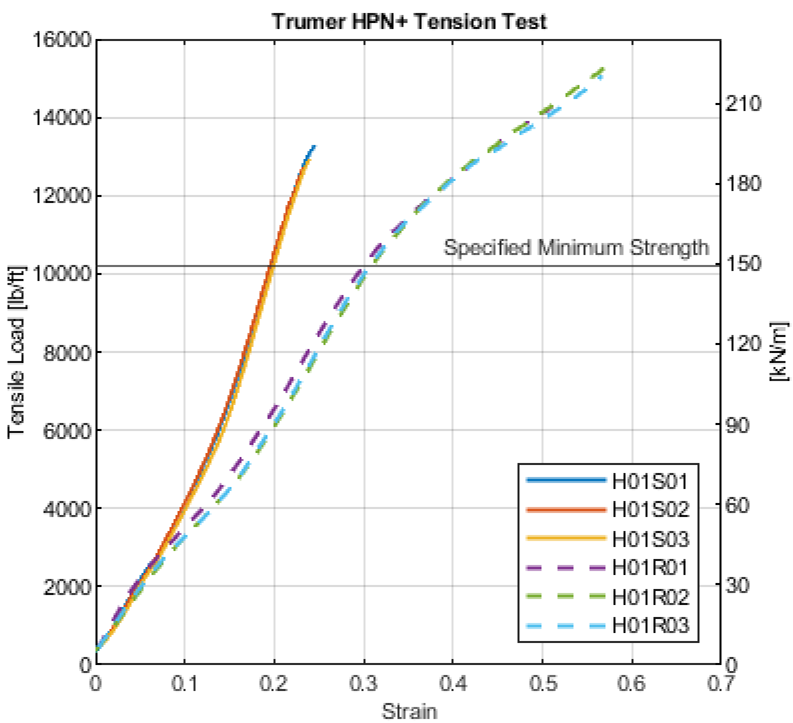


Figure 9. Trumer HPN+ load vs displacement

### 5.5. *Trumer Sigma Tension Test Results*

Trumer Sigma (Sigma) specimens were tested at a 3-cell loading length and Figure 10 presents the test data for both orientations. All tests completed passed specified minimum strength thresholds. A reduction in stiffness is not apparent in the load-displacement curve and can be accounted for in geometry as all curvature is limited to the nodes, similar to the Tecco mesh.

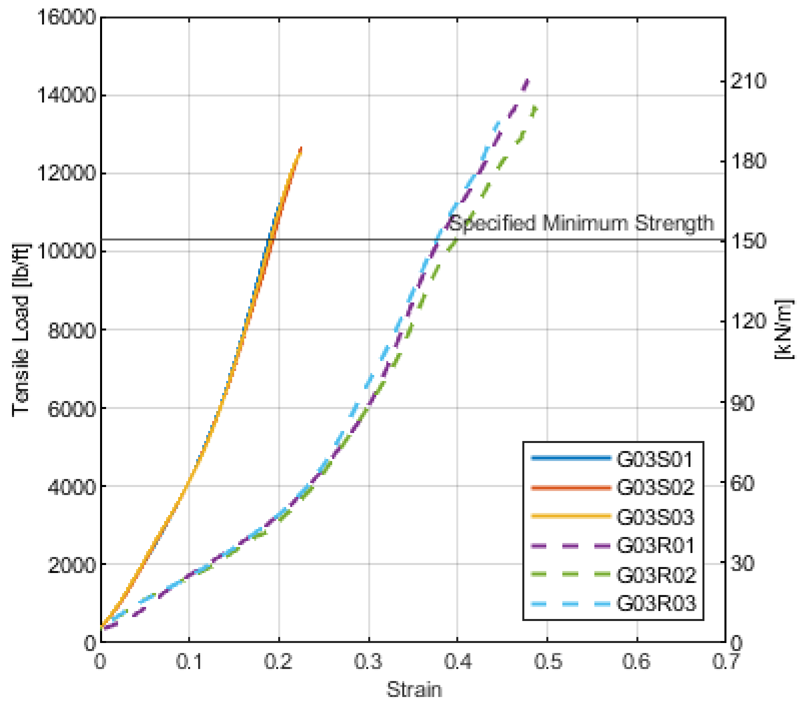


Figure 10. Trumer Sigma load vs displacement

## 6. Failure Modes

Under loading, mesh samples would undergo uniform elongation across the loading width until a distinct wire break corresponding with a significant drop in loading. After the initial break, the specimen would display an uneven elongation pattern with a widening on the side of the break. Initial breaks consistently occurred along the load path into the testing cell. After the initial break, the mesh would stabilize under the new geometry and loading would then increase to values less than the Ultimate Tensile Loading (UTL) before undergoing a secondary break. An example of the full loading sequence is shown in Figure 11.

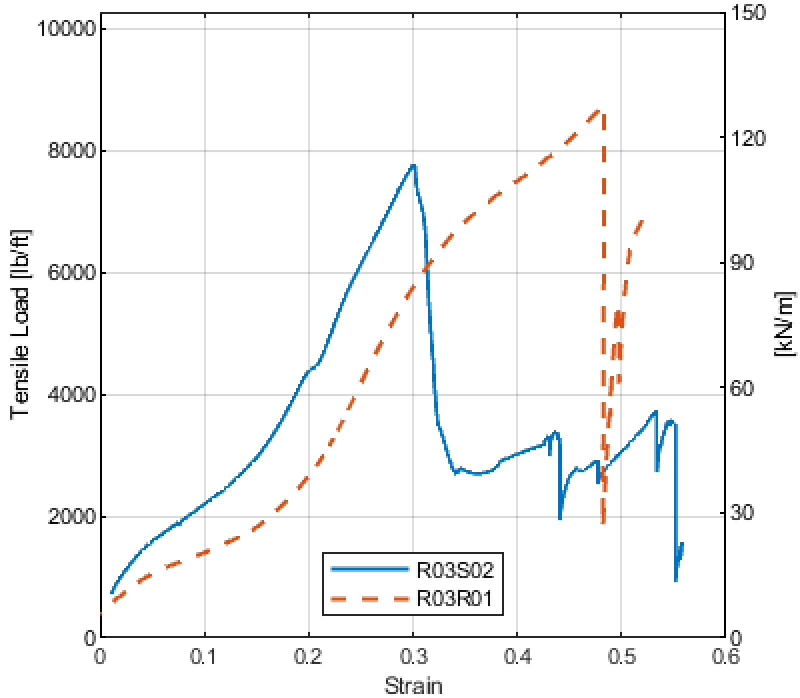


Figure 11. Typical load vs displacement after initial failure (SSM shown)

Failure locations were associated with the geometry of the sample. Two main initial failure locations were observed with the most common being a wire connecting the testing cell to an assembly bolt close to the center of the mesh sample as viewed in Figure 12 (a) and Figure 12 (c). When breaking at this location, the loading would correspond to the UTL and breaks beyond this point, viewed in Figure 12 (e) would correspond to a reduction in loading.

The second location of initial failure was at the outermost loaded wire from the boundary condition as viewed in Figure 12 (b) and Figure 12 (d). When breaking at this location, the sample would reach a higher load at the second beak of the sample, which can be viewed in Figure 12 (e), corresponding to the first failure location described above.

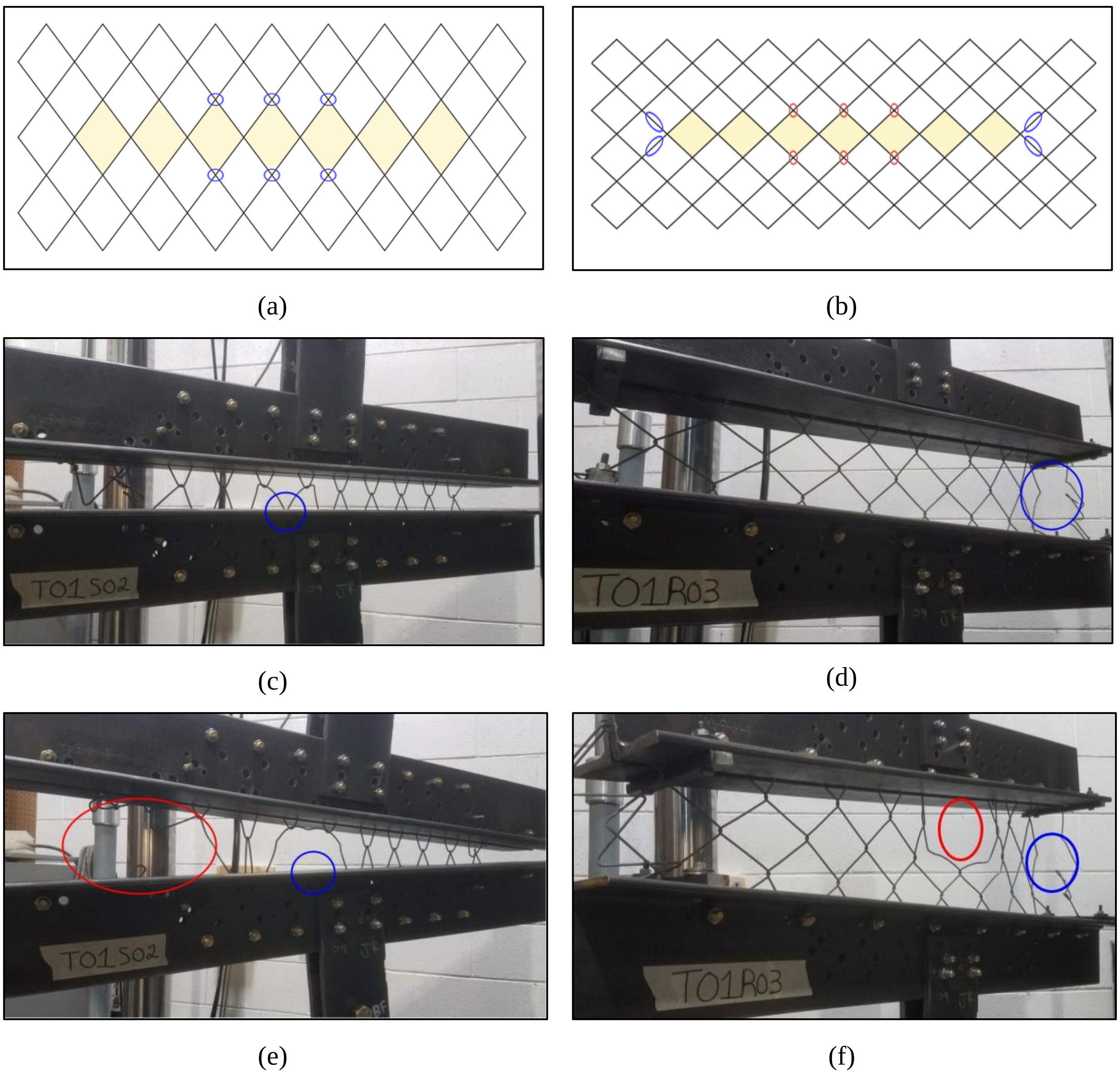


Figure 12. Typical locations of (a) type I and (b) type II failures with initial locations highlighted in blue (c) and (d), and secondary failures highlighted in red (e) and (f).

Specimens that saw an initial break that did not correspond with the UTL can be described as single-twist mesh with a single-cell width much greater than the single-cell length. A higher Poisson's effect due to the increased strain along the loading width is thought to be the cause of the failure. This failure mode was not present in Doubletwist mesh due to the ability of the Doubletwist connection to deform and reduce overall strain in corner boundaries under loading.

## 7. Comparison of Mesh Tensile Testing

Mesh samples are compared through measures of Ultimate Tensile Loading (UTL) and modulus of elasticity, measured as the UTL divided by the corresponding strain and neglecting the depth of mesh. This information is shown graphically in Figure 13. In this representation, and ideal mesh with a high modulus of elasticity and high UTL will be found in the upper right corner of the graph. All load-displacement curves have been averaged and plotted in Figure 14 (a) with subplots of standard orientation specimen found in Figure 14 (b) and rotated orientation specimen in Figure 14 (c).

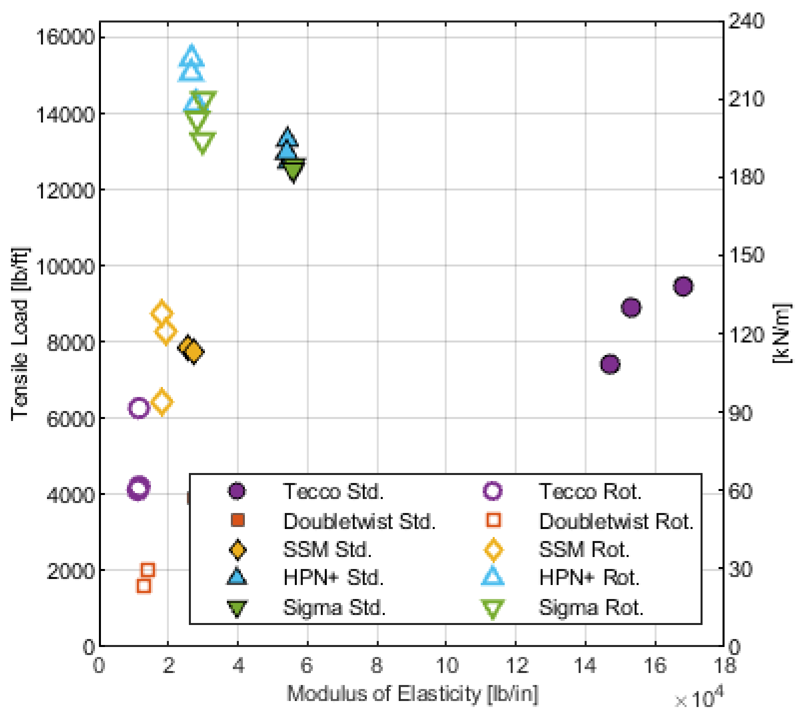


Figure 13. CU Boulder CIEST tension test results

University of Colorado Boulder
Center for Infrastructure, Energy, & Space Testing

Dept. of Civil, Environmental & Architectural Engineering
College of Engineering and Applied Science
428 UCB
Boulder, Colorado 80309-0428

t: 303.492.8221
CIEST@colorado.edu
website:www.colorado.edu/center/ciest

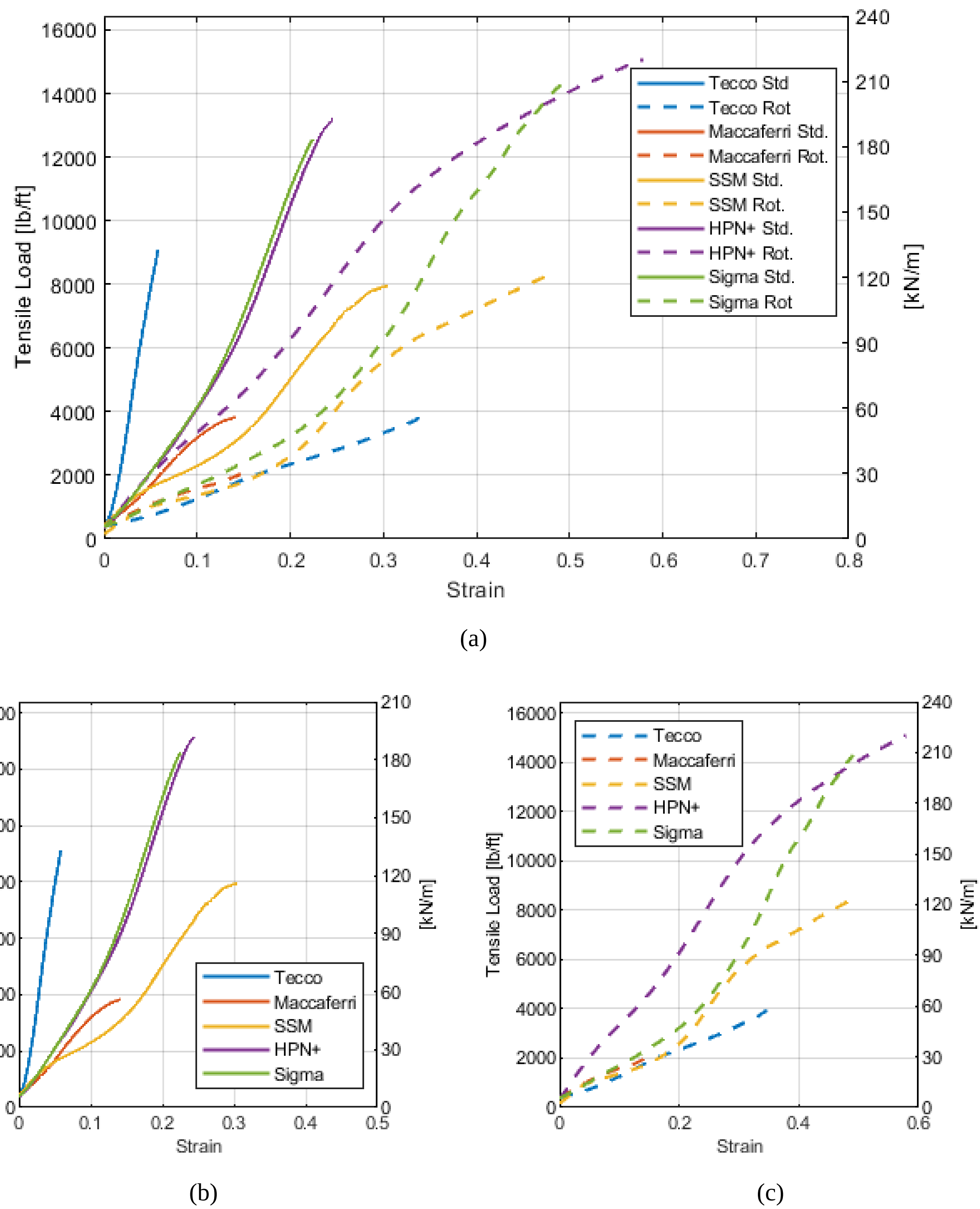


Figure 14. Comparison of Stress-Strain Curves of (a) All Tests, (b) Standard Orientation Tests, and (c) Rotated Orientation Tests

Dept. of Civil, Environmental & Architectural Engineering
College of Engineering and Applied Science
428 UCB
Boulder, Colorado 80309-0428
t: 303.492.8221
CIEST@colorado.edu
website:www.colorado.edu/center/ciest

Several observations can be made about the effect of the mesh geometry on the stress-strain curves. The stiffness of a mesh is correlated to the length/width ratio of the mesh cell. As the length to width ratio of the mesh cell increases, the modulus of elasticity along the strong axis will increase and modulus of elasticity along the weak axis will decrease. It is apparent that the curvature of wire through the node of the mesh is correlated to the reduced stiffness section of the load-displacement response and can be roughly measured as the depth of the mesh. When comparing mesh with similar wire diameter such as SSM, Tecco, Doubletwist, and Sigma, a greater depth of the mesh corresponded to a larger section of reduced stiffness. As curvature in the nodes is decreased, increasing the overall depth of the mesh, modulus of elasticity will be reduced due to displacement along the axis normal to the plane of loading.

Table 2. Comparison of Ultimate Tensile Load of mesh specimen and orientation

| **Specimen** | **Average Strain at UTL** | **Average Ultimate Tensile Loading lb/ft (kN/m)** | **Modulus of Elasticity (lbs/in)** |
|---|---|---|---|
| Soil Stabilization Mesh standard orientation | 0.284 | 7940 (115) | 2330 |
| Soil Stabilization Mesh rotated orientation | 0.425 | 7820 (114) | 1530 |
| Maccaferri Doubletwist standard orientation | 0.136 | 3810 (55.6) | 2340 |
| Maccaferri Doubletwist rotated orientation | 0.136 | 1820 (23.2) | 1120 |
| Geobrugg Tecco standard orientation | 0.0550 | 8600 (125) | 13000 |
| Geobrugg Tecco rotated orientation | 0.546 | 4860 (70.9) | 743 |
| Trumer HPN+ standard orientation | 0.240 | 13000 (189) | 4530 |
| Trumer HPN+ rotated orientation | 0.552 | 14900 (217) | 2250 |
| Trumer Sigma standard orientation | 0.224 | 12500 (182) | 4660 |
| Trumer Sigma rotated orientation | 0.471 | 13800 (201) | 2450 |

A comparison of strength and modulus of elasticity values completed by different labs can be viewed in Figure 15. Standard orientation UTL measurements completed by CIEST of Geobrugg Tecco G65 correlate well with testing completed by WMEL while Ruegger Systems reported higher values. The greater UTL values achieve by Ruegger Systems can be attributed to differences in test design such as the use of flexible boundary restraints that allow for greater stress redistribution throughout the mesh compared to the rigid restraints used by CIEST and WMEL. Standard orientation Doubletwist UTL measurements from CIEST align well with measurements from WMEL. Measurements from both CIEST and WMEL testing for Maccaferri Doubletwist are above minimum values specified on the certified data sheet while strength values of Geobrugg Tecco G65 were consistently below certified minimum strength values.

Standard orientation Geobrugg Tecco G65 modulus of elasticity values were higher than those reported by WMEL while correlating well with values reported by Ruegger Systems. As a lower prestress value under identical testing methods would either have no effect or lower the modulus of elasticity of a given mesh, it would follow that the test design of the EN 10223-3 tension test inherently produces higher modulus of elasticity values than that of ASTM A975. Modulus of Elasticity values for standard orientation Maccaferri Doubletwist were lower than those reported by WMEL.

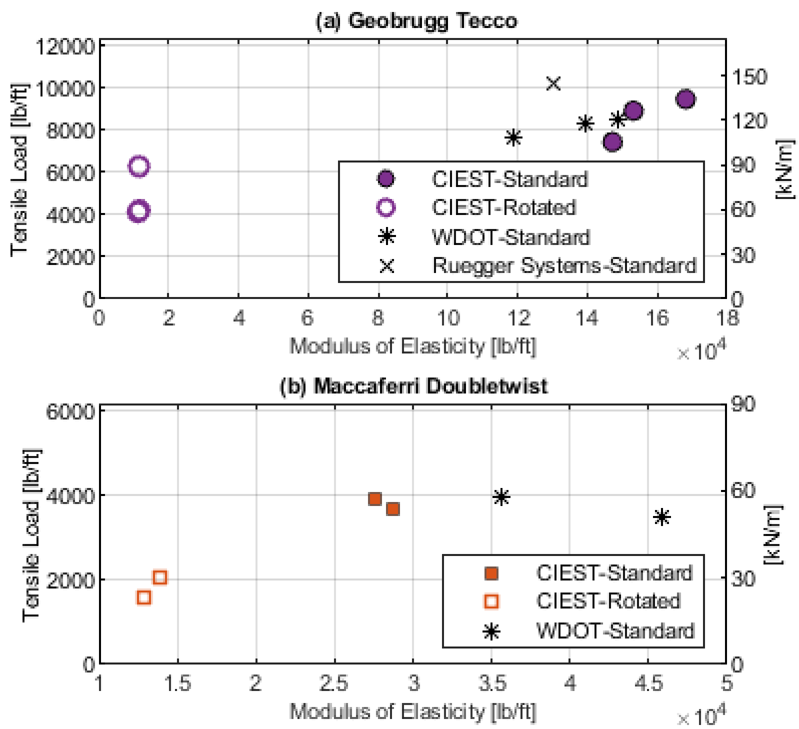


Figure 15. Comparison of tension tests to previous testing results for (a) Geobrugg Tecco and (b) Maccaferri Doubletwist meshes

Dept. of Civil, Environmental & Architectural Engineering
College of Engineering and Applied Science
428 UCB
Boulder, Colorado 80309-0428
t: 303.492.8221
CIEST@colorado.edu
website:www.colorado.edu/center/ciest

## Appendix

This appendix provides information focused on the geometries of each mesh tested. Mesh samples have been photographed in the standard orientation as defined in manufacturer specifications as well as the associated cross-section displaying the mesh depth. Reported dimensions are averaged measurements taken on each specimen tested. Individual width and height measurements were taken as 1/3 of a three-cell length.

Table 3. Overview and Dimensions of Tested Specimens

| **Description** | **Single-Cell Dimensions ($L_{1C}$ x $B_{1c}$) in. [mm]** | **Mesh Depth in. [mm]** |
|---|---|---|
| Soil Stabilization Mesh, standard orientation | 3 x 2 [76 x 50.8] | 0.71 [18] |
| Soil Stabilization Mesh, rotated orientation | 2 x 3 [50.8 x 76] | 0.71 [18] |
| Maccaferri GALMAC-Coated Terramesh, standard orientation | 5.67 x 3.26 [144 xx 88] | 0.12 [3] |
| Maccaferri GALMAC-Coated Terramesh, rotated orientation | 3.26 x 5.67 [88 x 144] | 0.12 [3] |
| Geobrugg Tecco G65, standard orientation | 5.63 x 3.26 [143 x 88] | 0.43 [11] |
| Geobrugg Tecco G65, rotated orientation | 3.26 x 5.63 [88 x 143] | 0.43 [11] |
| Trumer HPN+, standard orientation | 3.73 x 3.40 [94 x 86] | 0.79 [20] |
| Trumer HPN+, rotated orientation | 3.40 x 3.73 [86 x 94] | 0.79 [20] |
| Trumer Sigma, standard orientation | 2.90 x 3.10 [74 x 79] | 0.67 [17] |
| Trumer Sigma, rotated orientation | 3.1 x 2.9 [79 x 74] | 0.67 [17] |

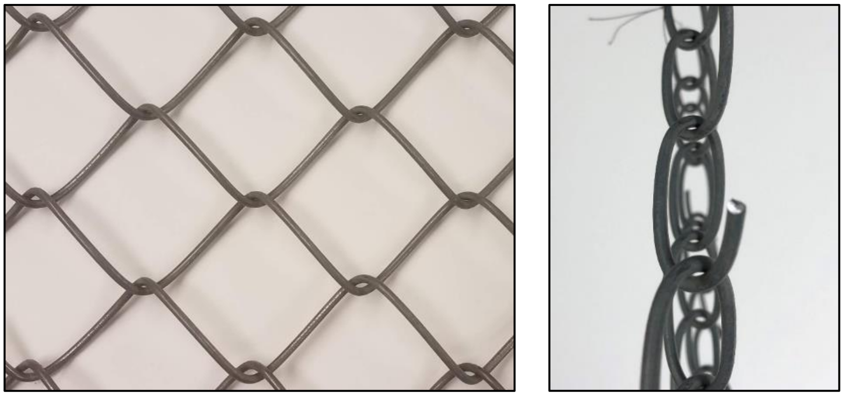

(a)

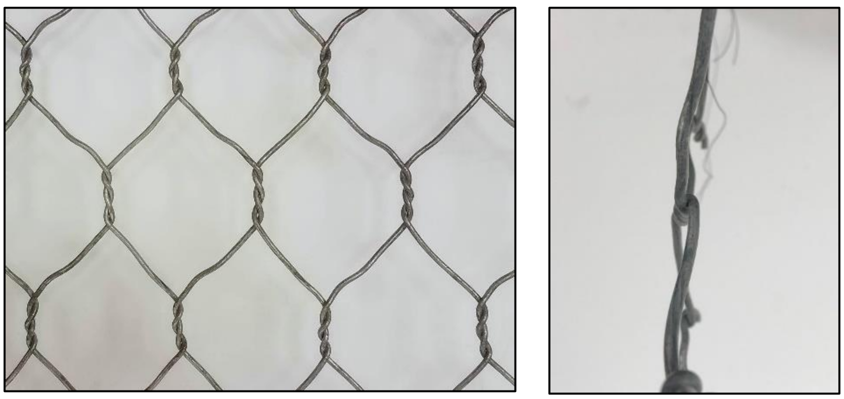

(b)

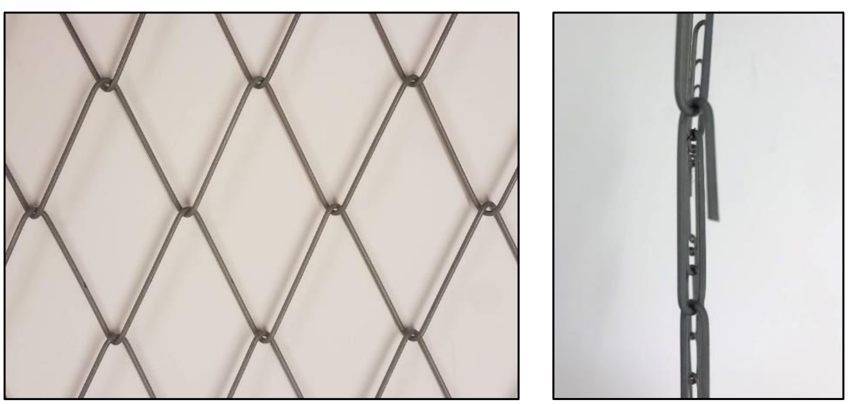

(c)

University of Colorado
Boulder
Center for Infrastructure, Energy, & Space Testing

Dept. of Civil, Environmental & Architectural Engineering
College of Engineering and Applied Science
428 UCB
Boulder, Colorado 80309-0428
t: 303.492.8221
CIEST@colorado.edu
website:www.colorado.edu/center/ciest

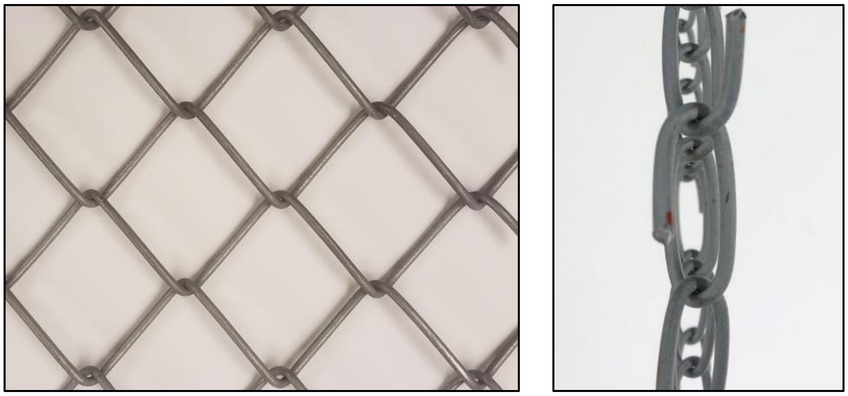

(d)

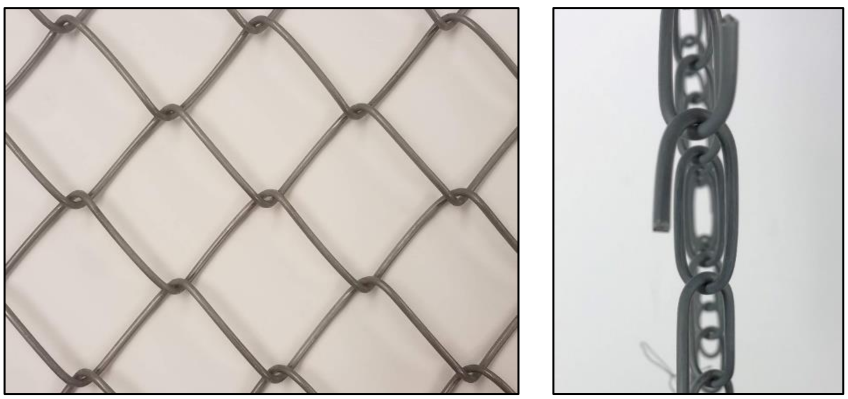

(e)

Figure 16. Wire Mesh Geometries and cross sections of (a) Soil Stabilization Mesh, (b) Maccaferri Doubletwist, (c) Geobrugg Tecco, (d) Trumer HPN+, and (e) Trumer Sigma

# References

ASTM International (2016) "Standard Specification for Double-Twisted Hexagonal Mesh Gabions and Revet Mattresses (Metallic-Coated Steel Wire or Metallic-Coated Steel Wire with Poly (Vinyl Chloride) (PVC) Coating)", *ASTM Standards. A975, 1-8.*

EN (2013) "Steel Wire and Wire Products for Fencing and Netting – Hexagonal Steel Wire Mesh Products for Civil Engineering Purposes" EN Standards. 10223-3, 1-24

European Assessment Document (2016) "Flexible Facing Systems For Slope Stabilization And Rock Protection" EAD 230025-00-0106

Bertolo P., Oggeri C., Peila D. (2009). "Full scale testing of draped nets for rock fall protection" Canadian Geotechnical Journal, No. 46 pp. 306-317.

Flum, D. (2002). Preliminary tests part I, 10th-20th April, 2002 carried out in the quarry 'Lochezen' above Walenstadt, Ruegger Systems Report 40 304 – 03, St. Gallen, Switzerland.

Giacchetti, G., Grimod , Alberto, & Cheer, D. (2011). Soil Nailing with flexible structural facing: design and experiences. Proceedings of the Second World Landslide Forum, 1–6.

J. J. del Coz Díaz , P. J. García Nieto , D. Castro Fresno & E. Blanco Fernández (2009) Non-linear analysis of cable networks by FEM and experimental validation, International Journal of Computer Mathematics, 86:2, 301-313, DOI: 10.1080/00207160801965339

Morton, E, Thompson, A, Villaescusa, E and Roth, A 2007. Testing and analysis of steel wire mesh for mining applications of rock surface support. 11th congress of the International Society for Rock Mechanics. Ribeiro e Sousa, Olalla and Grossman (ed). Vol.2, July, pp. 1061 - 1064.